

STUDY OF THE BLUETOOTH HEADSET ANTENNA WITH THE USER'S HEAD

Kin-Lu Wong,¹ Ming-Ren Hsu,¹ Wei-Yu Li,¹ Saou-Wen Su,^{1,2} and Austin Chen²

¹Department of Electrical Engineering
National Sun Yat-Sen University
Kaohsiung 804, Taiwan

²Technology Research and Development Center
Lite-On Technology Corp.
Taipei 114, Taiwan

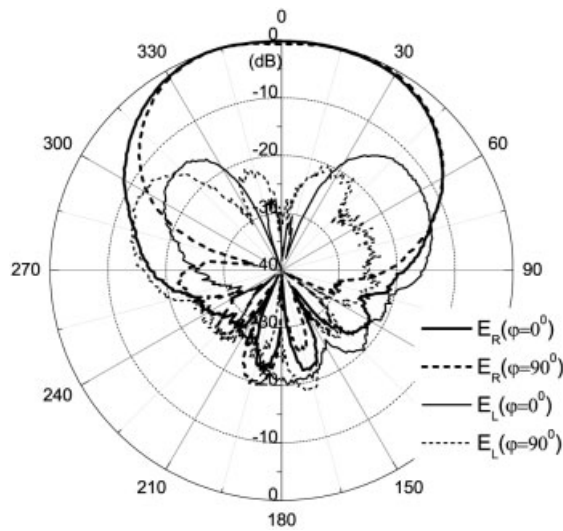


Figure 6 Measured patterns of the antenna at frequency 2.48 GHz with $a = 2^\circ$, and $h = 16$ mm

axial length of the helix with pitch angle 0.6 is 15% smaller than helix with pitch angle 4° in Ref. 5. The axial ratio as a function of the straight wire length is computed, and the current distribution and input impedance is given. The experimental results agree well with the simulation data, and the low profile and high polarization purity characteristics make the antenna suitable to form an array antenna in the satellite communications.

ACKNOWLEDGMENT

The authors acknowledge the financial support of the Hong Kong SAR research grant council via grant no. 9040934.

REFERENCES

1. J. Kraus, Antennas for all applications, 3rd ed., Mc Graw Hill, 2002.
2. U.R. Kraft and G. Monich, Main-beam polarization properties of modified helical antennas, IEEE Trans Antennas Propagat 38 (1990), 589–597.
3. H. Nakano, Y. Samada, and J.Yamauchi, Axial mode helical antennas, IEEE Trans Antennas Propagat 34 (1986), 1143–1148.
4. H.E. King and J.L. Wong, Characteristic of 1 to 8 wavelength uniform helical antennas, IEEE Trans Antennas Propagat 28 (1980), 291–296.
5. H. Nakano, H. Takeda, T. Honma, H. Mimaki, and J. Yamauchi, Extremely low-profile helix radiating a circularly polarized wave, IEEE Trans Antennas Propagat 39 (1991), 754–756.

© 2006 Wiley Periodicals, Inc.

Received 22 May 2006

ABSTRACT: A promising planar inverted-F metal-strip antenna suitable for Bluetooth headset application is studied. The antenna has a low-profile appearance and can be embedded inside the housing of the Bluetooth headset to operate as an internal antenna. The antenna is to be mounted along the side edge of the system circuit board of the headset, almost not occupying the valuable board space. Results have indicated that, when the antenna is mounted at either end of the side edge, a large bandwidth (>250 MHz) centered at about 2442 MHz can be achieved, making the antenna easily cover the Bluetooth operation in the 2400–2484 MHz band. Performances of the studied antenna attached to the user's head are also studied. Large distortion in the antenna's radiation pattern is observed. However, the antenna's radiation efficiency is still larger than about 70% over the operating band, which is acceptable for practical applications. Details of the obtained experimental and simulation results are presented and discussed. © 2006 Wiley Periodicals, Inc. Microwave Opt Technol Lett 49: 19–23, 2007; Published online in Wiley InterScience (www.interscience.wiley.com). DOI 10.1002/mop.22047

Key words: antennas; Bluetooth antennas; mobile antennas; Bluetooth headsets; user's head

1. INTRODUCTION

The Bluetooth headset for the mobile phone is recently becoming very attractive for wireless users. With the use of the Bluetooth headset, whose transmitted power is much less than that of the mobile phone, the possible absorption of the transmitted power for mobile communication by the user's head can be greatly reduced. For this application, we present in this paper a promising internal antenna suitable for application in the headset for covering the Bluetooth operation in the 2400–2484 MHz band. The antenna is a low-profile planar inverted-F metal-strip antenna [1–4] to be mounted along the side edge of the system circuit board of the headset, making it almost not occupying the valuable board space. With this arrangement, it is found that the achievable impedance bandwidth of the antenna is strongly dependent on the antenna's various positions along the side edge. The optimal position of the antenna for obtaining the maximal achievable bandwidth is found to be at either end of the side edge, and the achievable bandwidth can be larger than 250 MHz, allowing the antenna to easily cover the Bluetooth operation. Performances of the studied antenna with the presence of the user's head are also analyzed. Detailed results of the radiation pattern and radiation efficiency of the antenna are presented and discussed.

2. PROPOSED BLUETOOTH HEADSET ANTENNA

Figure 1 shows the configuration of the planar inverted-F metal-strip antenna mounted at the side edge of the system ground plane of the Bluetooth headset. The ground plane is printed on the back side of a 0.8-mm thick FR4 substrate of size 15×46 mm², which is treated as the system circuit board of the Bluetooth headset in the study. The selected size of the FR4 substrate is also about that

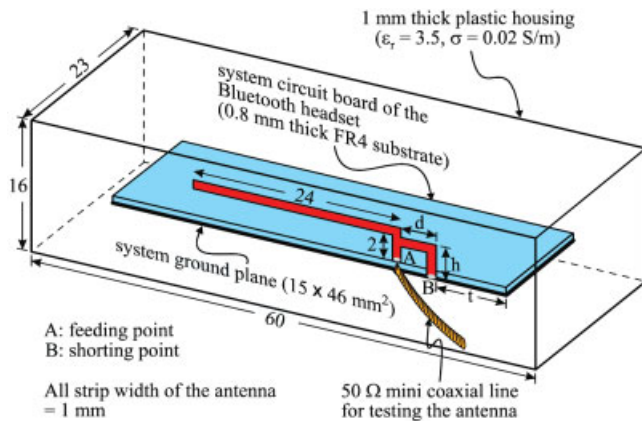


Figure 1 Configuration of the Bluetooth headset antenna for 2.4 GHz band operation. [Color figure can be viewed in the online issue, which is available at www.interscience.wiley.com]

of general Bluetooth headsets. Note that the FR4 substrate is enclosed by a 1-mm thick plastic housing of size $16 \times 23 \times 60 \text{ mm}^3$, which is treated as the housing of the Bluetooth headset.

The inverted-F metal-strip antenna is fabricated from a 0.2-mm thick copper plate in the study. No bending in the antenna structure is required, which makes the antenna easy to fabricate with a low cost. The antenna mainly comprises a radiating strip and a short-circuiting strip. The widths of the two strips are all set to be 1 mm. The length of the radiating strip starting from point A (the feeding point) is about 26 mm, which is close to a quarter-wavelength of the desired center frequency (2442 MHz) of the 2.4 GHz band. With the selected length of the radiating strip, a quarter-wavelength resonant mode can be excited at frequencies close to 2442 MHz for Bluetooth operation. Also, the radiating strip has a small height of 3 mm above the FR4 substrate or system circuit board, thus making the antenna have a low profile of 3 mm only.

For the short-circuiting strip, it is of an inverted-L shape and has a height of h and a lateral length of d . One end of the short-circuiting strip is connected to the system ground plane at point B (the shorting point), and the other end is connected to the radiating strip. By adjusting the dimensions of h and d , good impedance matching of the antenna over the excited resonant mode can be obtained.

It should also be noted that the achievable bandwidth of the excited resonant mode is greatly dependent on the position of the antenna along the side edge of the system ground plane. The position of the antenna in this design is defined by the distance t , which is the distance of the antenna's short-circuiting strip to one end of the side edge. It is expected that, when the antenna is placed at either end of the side edge of the system ground plane (that is, $t = 0$), a lower quality factor of the excited resonant mode can be obtained [5]. In this case, a wider bandwidth can be obtained for the antenna. The achievable bandwidth as a function of t will be discussed in more detail with the aid of Figure 3 in Section 3.

Furthermore, for considering the real environment of the proposed Bluetooth headset antenna in practical applications, the antenna with the presence of the user's head is included in the study (see the simulation model shown in Fig. 6 and the experimental photo shown in Fig. 7). Detailed user's head effects on the antenna performances will be analyzed with the aid of Figures 8–10 in Section 3. Also note that, for testing the antenna in the study, a 50-Ω mini-coaxial line is used, with its central conductor and outer grounding sheath connected to the feeding point and the system ground plane, respectively.

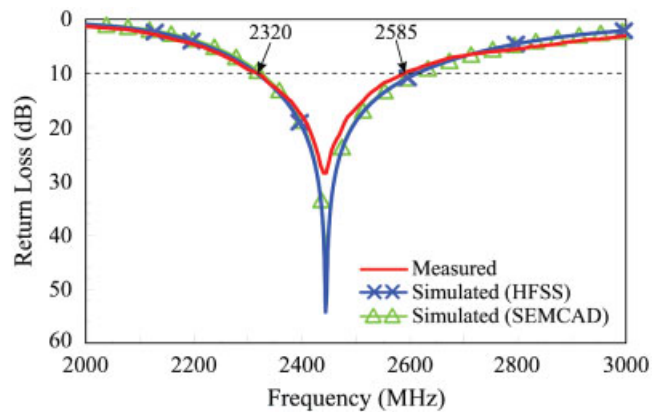


Figure 2 Measured and simulated return loss for the antenna shown in Figure 1 with $t = 0$, $d = 4.0 \text{ mm}$, $h = 3.8 \text{ mm}$. [Color figure can be viewed in the online issue, which is available at www.interscience.wiley.com]

3. RESULTS AND DISCUSSION

The proposed Bluetooth headset antenna was constructed and tested. Figure 2 shows the measured and simulated return loss for the constructed antenna. Note that the antenna is first placed at the end of the side edge (i.e., $t = 0$) for achieving a maximal operating bandwidth, and the 1-mm thick plastic housing enclosing the antenna is included in the study. For $t = 0$, the short-circuiting strip with $d = 4.0 \text{ mm}$ and $h = 3.8 \text{ mm}$ is selected for achieving good impedance matching over the excited resonant mode. It is first seen that the measured data agree well with the simulated results, which are obtained from Ansoft simulation software HFSS (high frequency structure simulator) [6] and the SPEAG simulation software SEMCAD (simulation platform for EMC, antenna design, and dosimetry) [7]. Defined by 10-dB return loss, the measured impedance bandwidth reaches as large as 265 MHz (2320–2585 MHz), which makes the antenna easily cover the 2.4 GHz band for Bluetooth operation.

To analyze the dependence of the achievable bandwidth of the antenna's excited resonant mode on the parameter t , a simulation study using Ansoft HFSS is conducted. Figure 3 shows the results for t varied from 0 to 18 mm. Note that, for the cases with t larger than 18 mm, the antenna's radiating strip will be extended out of the system ground plane, unless the radiating strip is bent to follow the boundary of the system ground plane. For this reason, the cases with t larger than 18 mm are not studied here. Also, for achieving

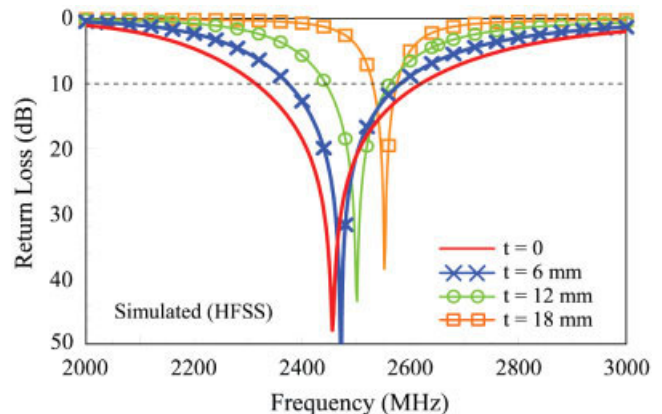


Figure 3 Simulated HFSS return loss for the antenna as a function of t ; other parameters are the same as in Figure 2. [Color figure can be viewed in the online issue, which is available at www.interscience.wiley.com]

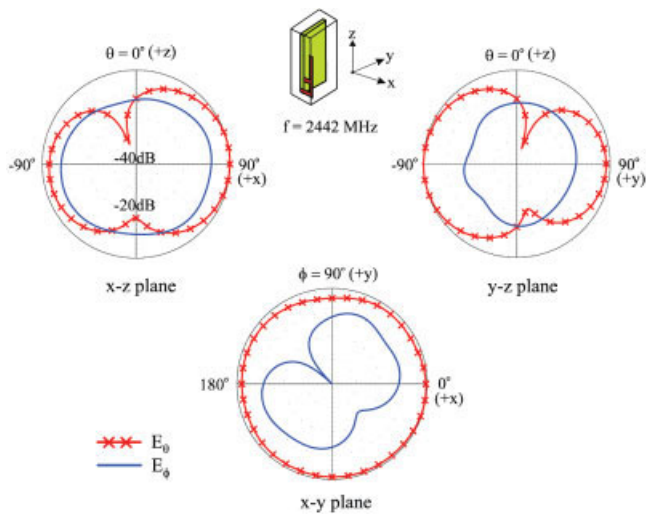


Figure 4 Measured radiation pattern at 2442 MHz for the antenna studied in Figure 2. [Color figure can be viewed in the online issue, which is available at www.interscience.wiley.com]

good impedance matching over the excited resonant mode, the parameter d are adjusted to be 2.9, 1.8, and 1.8 mm for $t = 6, 12,$ and 18 mm, respectively, and the corresponding values for the parameter h are adjusted to be 3.8, 3.8, and 2.1 mm. From the obtained results, it is seen that the impedance bandwidth is quickly decreased with an increase in t . The obtained bandwidths are about 300, 200, 120, and 40 MHz when the parameter t is 0, 6, 12, and 18 mm, respectively. Thus, in order to achieve a maximal bandwidth, the antenna should be placed at either end of the side edge of the system ground plane in the proposed design.

Figure 4 plots the measured radiation patterns at 2442 MHz for the constructed antenna with $t = 0$. Note that the radiation patterns shown in the three principal planes are normalized with the same amplitude. The obtained radiation patterns thus indicate that the antenna's maximal radiation power in the three principal planes is about the same. In addition, in the x - y plane, the antenna is seen to have near-omnidirectional radiation. The measured antenna gain and the simulated radiation efficiency obtained using Ansoft HFSS are also presented in Figure 5. Over the 2.4 GHz band for Bluetooth operation, the antenna gain level is about 2.5 dB and good radiation efficiency of larger than 90% is obtained.

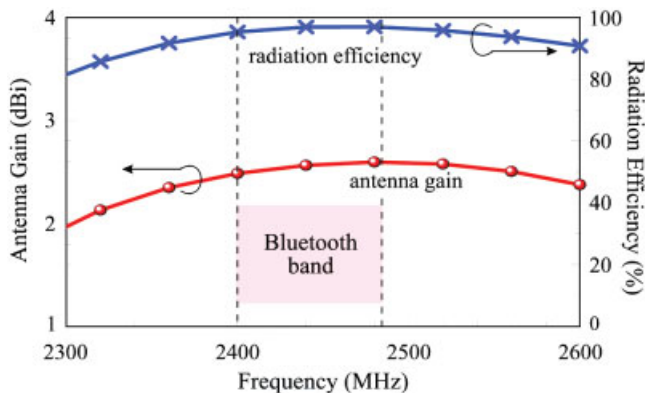


Figure 5 Measured antenna gain and simulated HFSS radiation efficiency for the antenna studied in Figure 2. [Color figure can be viewed in the online issue, which is available at www.interscience.wiley.com]

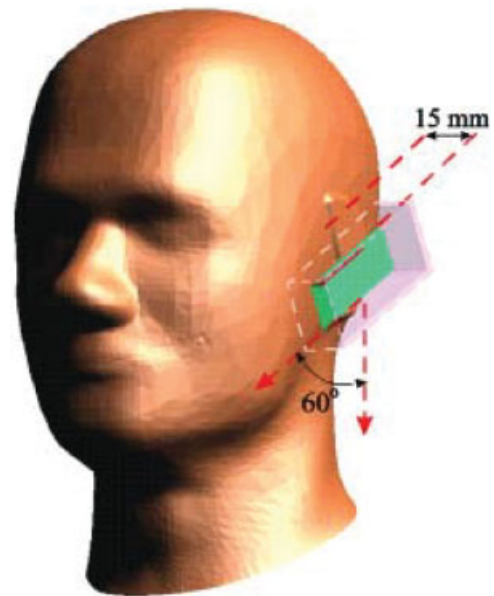


Figure 6 The studied Bluetooth headset antenna with the simulation head model provided by SEMCAD. [Color figure can be viewed in the online issue, which is available at www.interscience.wiley.com]

The user's head effects on the performances of the antenna are then studied. The studied Bluetooth headset antenna attached to the simulation head model provided by SEMCAD [7] is shown in Figure 6. As shown in the figure, the antenna is inclined to the vertical axis of the head model with an inclination angle of 60° , which is close to the general operation condition of the Bluetooth headset. In addition, the distance between the system ground plane and the head model is set to be 15 mm, which is also a reasonable distance for practical Bluetooth headset applications. Figure 7 shows the photo of the constructed Bluetooth headset antenna attached to a user's head in the experiment. The measured and simulated (SEMCAD) results of the return loss are presented in



Figure 7 Photo of the constructed Bluetooth headset antenna attached to a user's head in the experiment. [Color figure can be viewed in the online issue, which is available at www.interscience.wiley.com]

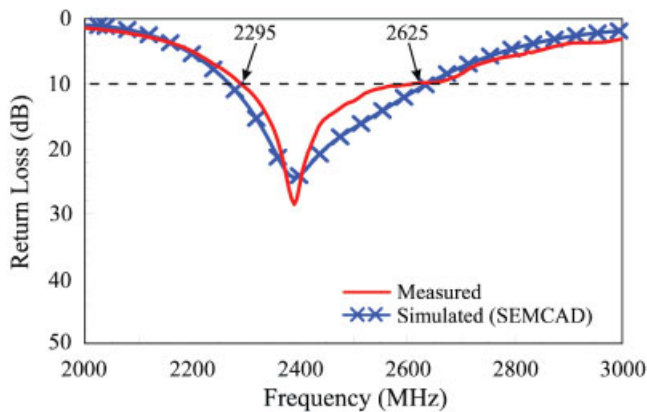


Figure 8 Measured and simulated (SEMCAD) return loss for the blue-tooth headset antenna with the user's head. [Color figure can be viewed in the online issue, which is available at www.interscience.wiley.com]

Figure 8 for comparison. Good agreement between the measurement and simulation is seen, which can ensure reliable simulated results obtained from SPEAG SEMCAD for the case with the user's head. Also, from the measured results, the 10-dB return-loss bandwidth reaches 330 MHz (2295–2625 MHz), which is larger than that for the case without the user's head (Fig. 2). This behavior indicates that the user's head can be treated as a lossy loading on the Bluetooth headset antenna. In this case, with the presence of the lossy loading, enhancement of the antenna's impedance bandwidth can be expected, however, with a sacrifice in the antenna's radiation efficiency [8, 9].

The simulated (SEMCAD) three-dimensional total-power radiation pattern at 2442 MHz for the antenna with the user's head is shown in Figure 9. Two radiation patterns of looking from the side face and the rear of the user's head are presented. It can be seen that there is large absorption of the radiation power in the direction of the user's head. On the contrary, maximal radiation power is obtained in the direction away from the user's head. Figure 10 shows the simulated (SEMCAD) radiation efficiency for the case with the user's head. As expected, a decrease in the antenna's radiation efficiency is seen. However, the radiation efficiency for frequencies over the 2.4 GHz band is still larger than about 70%, which is acceptable for practical applications.

4. CONCLUSION

A planar inverted-F metal-plate antenna suitable for application in Bluetooth headsets has been proposed and studied. Owing to its planar and simple structure, the proposed antenna is easy to fabricate with a low cost. Performances of the proposed antenna with the presence of the user's head have also been studied. Results first indicate that, with the proposed antenna placed at either end of the side edge of the system ground plane, a maximal operating bandwidth of larger than 250 MHz can be obtained. This large bandwidth allows the antenna to easily cover the 2.4 GHz band for Bluetooth operation. Conversely, when the short-circuiting position of the antenna is at the positions away from either end of the side edge, the achievable bandwidth can be as low as about 40 MHz only, making the antenna difficult to cover the Bluetooth operation. Large user's head effects on the performances of the antenna have also been observed. Large radiation power absorption in the direction of the user's head has been seen, which leads to large distortions in the antenna's radiation patterns. Although there is radiation power absorption owing to the presence of the user's head, the antenna's radiation efficiency is still better than

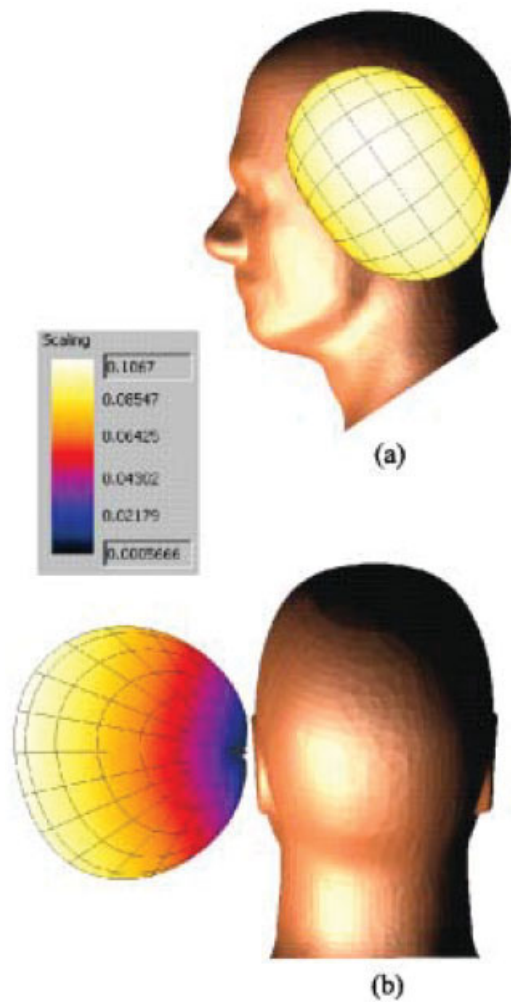


Figure 9 Simulated (SEMCAD) three-dimensional total-power radiation pattern at 2442 MHz for the antenna studied in Figure 2 with the user's head. (a) Looking from the side face of the user's head. (b) Looking from the rear of the user's head. [Color figure can be viewed in the online issue, which is available at www.interscience.wiley.com]

70% over the operating band. The obtained performances make the proposed antenna very promising for practical Bluetooth headset applications.

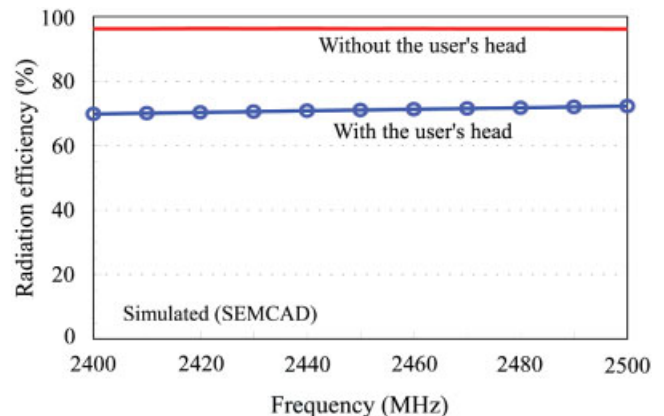


Figure 10 Simulated (SEMCAD) radiation efficiency for the antenna studied in Figure 2 with the user's head. [Color figure can be viewed in the online issue, which is available at www.interscience.wiley.com]

REFERENCES

1. K.L. Wong, Planar antennas for wireless communications, Wiley, New York, 2003, Chapter 5.
2. C.M. Su and K.L. Wong, Narrow flat-plate antenna for 2.4 GHz WLAN operation, *Electron Lett* 39 (2003), 344, 345.
3. C.M. Su, W.S. Chen, Y.T. Cheng, and K.L. Wong, Shorted T-shaped monopole antenna for 2.4/5 GHz WLAN operation, *Microw Opt Technol Lett* 41 (2004), 202, 203.
4. K.L. Wong, L.C. Chou, and C.M. Su, Dual-band flat-plate antenna with a shorted parasitic element for laptop applications, *IEEE Trans Antenn Propag* 53 (2005), 539–544.
5. J. Villanen, J. Ollikainen, O. Kivekas, and P. Vainikainen, Compact antenna structures for mobile handsets, In: *Proceedings of IEEE 58th Vehicular Technology Conference*, Vol. 1, 2003, pp. 40–44.
6. <http://www.ansoft.com/products/hf/hfss/>, Ansoft corporation HFSS.
7. <http://www.semcad.com>, SEMCAD, Schmid & Partner Engineering AG (SPEAG).
8. K.L. Wong, Compact and broadband microstrip antennas, Wiley, New York, 2002, Chapter 3.
9. K.L. Wong and Y.F. Lin, Small broadband rectangular microstrip antenna with chip-resistor loading, *Electron Lett* 33 (1997), 1593–1594.

© 2006 Wiley Periodicals, Inc.

THE ROBUST DESIGN FOR GAPLESS MICROLENS ARRAY FABRICATION USING THE INCOMPLETE DEVELOPING AND THERMAL REFLOW PROCESS

Shih-Yu Hung,¹ Shih-Nung Chen,¹ Che-Ping Lin,¹ and Hsiharng Yang²

¹Department of Automation Engineering
Nan Kai Institute of Technology
Tsaotun

Nantou 542, Taiwan

²Institute of Precision Engineering
National Chung Hsing University
Taichung 402, Taiwan

Received 22 May 2006

ABSTRACT: A systematic approach to achieving high quality gapless microlens array fabrication using the incomplete developing and thermal reflow process was developed in this study. The experimental results proved that a hexagonal microlens array with a maximum 100% fill-factor could be successfully produced. The major objective in using this robust design is to reduce the variations in microlens array focal length, allowing improved focus and enhanced illumination brightness. In this experiment, the Taguchi method was used first to perform an efficient experimental design and analyze the robustness of the microlens array fabrication process. Several parameters affect microlens array uniformity; the hexagonal column diagonal, spin coating revolution speed, exposure time, developing time, and reflow temperature. It is very important to control these parameters to decrease the sensitivity to noise. Therefore an artificial neural network (ANN) was used to minimize the variation and make the microlens array less sensitive to process variation. The L_{18} orthogonal array was used as the learning data for the ANN to construct an ANN model that could predict the parameters at nondiscrete levels. The results showed the microlens array quality was significantly improved compared with the original design. © 2006 Wiley Periodicals, Inc. *Microwave Opt Technol Lett* 49: 23–29, 2007; Published online in Wiley InterScience (www.interscience.wiley.com). DOI 10.1002/mop.22046

Key words: microlens array; robust design

1. INTRODUCTION

During the past few years, the major microlens array application has been enhancing the illumination brightness and simplifying light-guide module construction. In a laptop display, a 25% increase in light output was reported when microlens technology was used [1]. The integrated microlens array is a very important part in CCDs, autofocus modules, copiers [2], and optical fiber interconnects [3]. Microlens arrays can be produced using various methods such as electron-beam lithography, photolithographic etching, hot embossing [4, 5], and thermal reflow. The thermal reflow technique is commonly used in refractive microlens arrays fabrication by melting cylindrical resist posts onto the substrate [6].

The lens shape and the fill-factor are two of many conditions that impact the overall light efficiency. To collect the maximum amount of light, the lens area must be as close to 100% of the total area as possible. The fill-factor is defined as the percentage of lens area to the total area. It is also referred to as the Strehl ratio [7]. The fill-factor is influenced by the pixel geometry and lens layout [8]. Most of the technical literature related to microlens fabrication discussed only round geometrical lenses. The fill-factor for a round microlens array was considered in orthogonal and hexagonally arranged arrays. In an orthogonal array (OA), the maximum fill-factor (assuming that no gap exists between the lenses) is 78%. In a hexagonally arranged array for a round microlens, the fill-factor is larger (about 90%). Lin et al. [9] and Yang et al. [10] presented a special fabrication process that used the incomplete developing technique to produce the hexagonal and square microlens array with a maximum fill-factor of nearly 100%. Furthermore, Lin et al. proposed a novel microlens array fabrication method [11] that controlled the printing gap in the UV lithography process. This method can precisely control the microlens geometric profile array in the fabrication process without thermal reflow.

The microlens array fabrication quality control is becoming more important as the microlens array area becomes larger. Considering the deviations in design variables in the early design stages is a recent trend in quality engineering. Microlens array quality should be accomplished by producing low cost and high performance by reducing the variation. The variations due to the raw material, manufacturing process parameters, and operation conditions would limit microlens array applications. Taguchi [12, 13] introduced the parameter design concept, which improves the quality of a product whose manufacturing process involves significant variability. However, Montgomery [14] pointed out that the Taguchi approach to experimental design is weak in dealing with the potential interactions between controllable factors. Taguchi's data analysis method may confound the location and dispersion effects.

An artificial neural network (ANN) is an information processing model that is inspired by the working of the brain. It is composed of a large number of highly interconnected processing elements (neurons) working in unison to solve specific problems. An ANN is configured for a specific application, such as pattern recognition or nonlinear system simulation, through a learning process. Rumelhart et al. [15] published the "back-propagation" algorithm, which showed that it was possible to train a multilayer neural architecture using a simple iterative procedure. In recent years, ANNs have been widely applied to model complex manufacturing process, generally for process and quality control [16]. This paper describes the effective application of Taguchi method for the design of neural networks [17], which can conform to the required accuracy and convergence speed. The objective of this work is to minimize the performance variability in the focal lengths for a hexagonal microlens array. This will allow the array to focus accurately on identical positions, enhancing the illumination brightness.